

## Modelling of wind wave-induced bottom processes during the slack water periods in Tampa Bay, Florida

John Z. Shi<sup>1,\*</sup>, Mark E. Luther<sup>2</sup> and Stephen Meyers<sup>2</sup>

<sup>1</sup>*School of Naval Architecture, Ocean and Civil Engineering, Shanghai Jiao Tong University,  
1954 Hua Shan Road, Shanghai 200030, China*

<sup>2</sup>*College of Marine Science, University of South Florida, 140 Seventh Avenue South, St. Petersburg,  
FL 33701, U.S.A.*

### SUMMARY

Estuarine process-oriented modelling studies were undertaken to understand bottom boundary layer processes in Tampa Bay, Florida. A stationary shallow water wave model, SWAN, was applied to predict wind wave-induced rms bottom orbital currents in Tampa Bay on a  $70 \times 100$  curvilinear grid. Simulations were performed by using two idealized wind forcing (i.e. northeasterly winds of 10 and  $20 \text{ m s}^{-1}$ ) and high-resolution bathymetry. Calculations of bed load and total load of fine sand were made by using the transport formulas of Van Rijn (*J. Hydraulic Eng.* 1984; **110**:1431–1456) and Engelund–Hansen (*A Monograph on Sediment Transport in Alluvial Streams*. Copenhagen Technical Press: 1972), respectively. Simulations of wind wave induced currents reveal that they are important for fine sand transport along the shallow margins of the Tampa Bay. Modelled bottom orbital currents ranged from 0.05 to  $0.39 \text{ m s}^{-1}$ . Total loads of fine sand ranged from  $2.26 \times 10^{-10}$  to  $1.05 \times 10^{-5} \text{ kg m}^{-1} \text{ s}^{-1}$  for northeasterly winds of  $10 \text{ m s}^{-1}$  and from  $2.46 \times 10^{-5}$  to  $3.21 \times 10^{-5} \text{ kg m}^{-1} \text{ s}^{-1}$  for northeasterly winds of  $20 \text{ m s}^{-1}$ . Wind wave-induced bottom resuspension is an important process affecting water quality in Tampa Bay. Copyright © 2006 John Wiley & Sons, Ltd.

Received 28 May 2006; Revised 14 August 2006; Accepted 16 August 2006

KEY WORDS: wind wave; bottom currents; fine sand transport; Tampa Bay

\*Correspondence to: John Z. Shi, School of Naval Architecture, Ocean and Civil Engineering, Shanghai Jiao Tong University, 1954 Hua Shan Road, Shanghai 200030, China.

†E-mail: zshi@sjtu.edu.cn

Contract/grant sponsor: Ministry of Education of People's Republic of China

Contract/grant sponsor: USGS Center for Coastal Geology and Regional Marine Studies; contract/grant number: 03QMH1408

Contract/grant sponsor: National Science Fund for Distinguished Young Scholars of China; contract/grant number: 40225014

## 1. INTRODUCTION

Wave boundary layer currents induce shear stresses that resuspend and transport materials from the sea floor [1]. Observations of tidal resuspension of estuarine cohesive sediments have been made in several estuaries or bays, e.g. the Chesapeake Bay, U.S.A. [2], and the Changjiang River estuary, China [3]. Wind waves have also been observed to resuspend and transport bottom non-cohesive sediments in the Long Island Sound [4], and the Chesapeake Bay, U.S.A. [5, 6]. Lou and Ridd [7] analysed wave–current bottom shear stresses and sediment resuspension in Cleveland Bay, Australia.

Modelling of estuarine and coastal cohesive and non-cohesive (sand) sediment resuspension and transport has been attempted by a number of researchers. For example, Mei and Chain [8] and Mei *et al.* [9] carried out theoretical studies of resuspension and transport of fine sand by waves. Lin and Falconer [10] carried out numerical modelling of 3D suspended sediment transport for the Humber River estuary, U.K. Booth *et al.* [11] derived an empirical model of wind-induced bottom sediment resuspension for the Barataria Basin, Louisiana, U.S.A. They found that winds of  $4 \text{ m s}^{-1}$  could resuspend approximately 50% by area of bottom sediments. Signell *et al.* [12] carried out a modelling study of bottom currents and sediment (medium sand) transport in the Long Island Sound, U.S.A.

Tampa Bay is a microtidal estuary incised into Tertiary platform carbonates [13]. As shown in Figure 1, it consists of the Old Tampa Bay, the Hillsborough Bay, the Middle Tampa Bay, and the Lower Tampa Bay [14]. Total Bay water area is about  $1009.67 \text{ km}^2$  with a mean depth of about 3.30 m [15]. Winds are generally from the northeast during the winter. Annual average wind speed is  $3.40 \text{ m s}^{-1}$  from the northeast. Tides are mixed, diurnal, and semidiurnal, with a mean range of about 0.67 m. The tidal range gradually increases from the mouth of the Bay to its upper reaches. Maximum tidal currents were less than  $0.15 \text{ m s}^{-1}$  in Old Tampa Bay [16]. The vertically-averaged currents in Tampa Bay during a typical flood tide were generally less than  $0.50 \text{ m s}^{-1}$  [17]. These may be attributed to the bottom topographic variations (or different water depth, Figure 2) and different weather conditions in the different parts of the Tampa Bay. No information is available for the wind-driven currents during the cold fronts in the literature. It is believed that a very strong wind would generate strong currents within this shallow Tampa Bay. Tampa Bay is well-mixed because of the shallow water depths, relatively small freshwater inflows, small range of tides, and effects of wind [15]. It exhibits horizontal salinity gradients, i.e. the horizontal variation of salinity from relatively fresh to relatively salty water between the estuary's head and the coastal ocean [18].

Knowledge of the characteristics of bottom sediment resuspension is critical for understanding the distribution and transformation of natural materials and contaminants in Tampa Bay. According to Florida Marine Research Institute, the Tampa Bay system, which has been highly developed and urbanized, has lost 81% of its seagrass acreage over the past 100 years. Studies have shown that wind wave-induced bottom currents and sand transport have physical, biological significances in water quality and eutrophication in Tampa Bay [14, 19] and seagrass meadows in Tampa Bay [20, 21].

Observations of hydrodynamics (wind waves, tides) and sediment resuspension have been carried out in Tampa Bay [16, 17, 19, 22, 23]. Modelling studies have also been attempted for describing tidal hydrodynamics and density-driven circulation in Tampa Bay: (1) two-dimensional horizontal (2DH) [15]; and (2) three-dimensional (3D) tidal hydrodynamic model for Tampa Bay [17, 24–28]. Three-dimensional (3D) density-driven circulation model was also developed for Tampa Bay [29].

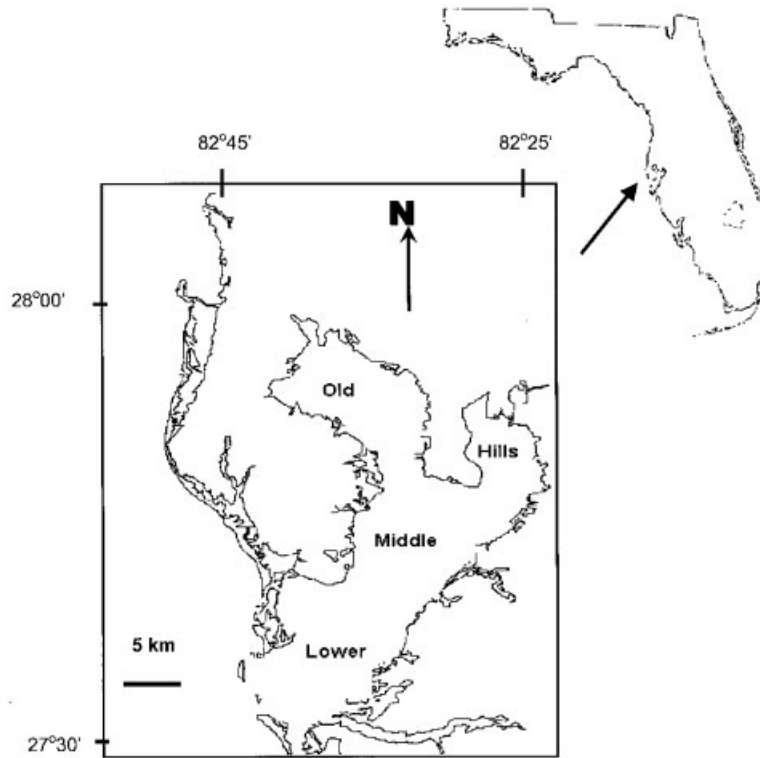


Figure 1. Tampa Bay, west-central Florida.

Two major findings regarding sediment transport can be obtained from those observational and modelling studies: (1) bottom sediments are non-cohesive silts and fine sands [13, 16, 22, 23]; (2) primary mechanism for non-cohesive sediment (sand) resuspension is wind waves in Tampa Bay [16, 17, 19, 22, 23]. In addition, four types of bottom currents contribute to fine sand transport: (a) tide-induced bottom currents, (b) wave-induced bottom currents, (c) wind wave-induced currents, and (d) density-induced currents. Fast-varying wave-induced pressure gradients are on the order of seconds. The horizontal slowly varying pressure gradients associated with tide, wind-induced and density-driven circulations (currents) are on the order of minutes. Wind waves are generated by winter storm systems and tropical storms. They have significant bottom currents, and would resuspend fine sand by their bottom wave orbital motions. Since the Tampa Bay is well-mixed and only exhibits horizontal salinity gradients, density-induced currents are less important to fine sand transport.

However, little modelling has been done for wind wave boundary layer dynamics and fine sand transport in Tampa Bay. One-dimensional vertical (1 DV) cohesive sediment transport modelling has been confined to the Hillsborough Bay [17, 19]. Types of bed sediments vary in the Old Tampa Bay, the Hillsborough Bay, the Middle Tampa Bay and the Lower Tampa Bay, but most sediments are non-cohesive fine sand [16]. Approximately 98% of the Bay sediment is non-cohesive, and we therefore chose to use a sediment transport formula that is suitable for non-cohesive

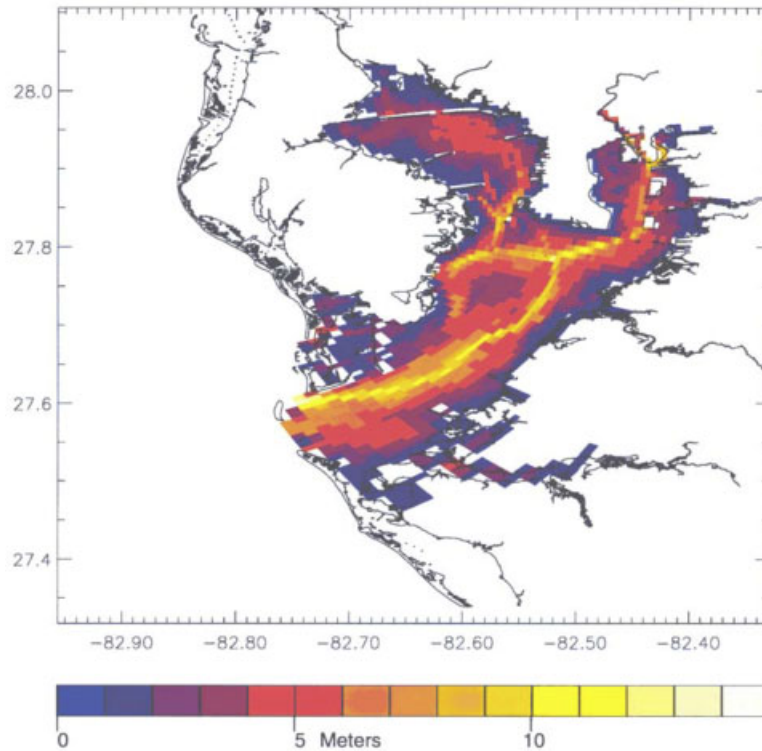


Figure 2. Bathymetry map of the Tampa Bay.

sediments. Little data on suspended sediment concentration is available for Tampa Bay. What are their relative contributions of bed load and suspended load of fine sand to sediment transport in Tampa Bay?

With these previous results in mind, the objectives of this work were to: (1) model wind waves-induced bottom orbital currents under two different idealized wind conditions; (2) calculate regional bed load and total load of fine sand under two different idealized wind conditions; and (3) examine dominant processes for fine sand transport in Tampa Bay. It should be noted that near bottom currents due to wave streaming velocities were included in this study. Preliminary results of an incomplete version were presented in [30].

## 2. WIND WAVE MODEL

Although both local and remote winds can drive currents in Tampa Bay, local winds are taken into account in this study. The patterns of bottom orbital currents in Tampa Bay were simulated with the numerical wave-prediction model *Simulating WAVes Nearshore (SWAN)*, that is being developed by the Delft University of Technology, The Netherlands. Detailed introductions into the background of SWAN can be found in Booij *et al.* [31]. The SWAN wave model is used for computing wind wave-induced bottom orbital velocity maximum  $U_b$  at each model grid cell under

two idealized wind conditions. The grid matches that used in an ECOM model of Tampa Bay [27, 28].

The numerical techniques in SWAN [32] were developed from those used in the second-generation HISWA model [33]. The discretized spectrum is partitioned into four quadrants, and a sequence of four forward marching sweeps is used to propagate the waves of each quadrant with an upwind finite difference scheme. This cycle is carried out iteratively, to allow boundary conditions to be matched between quadrants and an equilibrium solution obtained [32, 34].

Generally, in estuarine and coastal waters, the development, selection and evaluation of better friction models would probably be the most important remaining wind wave-induced bottom processes problem. Therefore, SWAN incorporates several bottom friction choices. For the sake of simplifications, the default choice of the friction models is selected in this paper. That is to say, in this study, the following friction models have been used for SWAN: (a) the empirical model of JONSWAP [35]; (b) the drag law model of Collins [36]; and (c) the eddy-viscosity model of Madsen *et al.* [37]. The formulations for those bottom friction models can all be expressed in the form

$$S_{ds,b}(\omega, \theta) = -C_b \frac{\omega^2}{g^2 \sinh^2(kd)} E(\omega, \theta) \tag{1}$$

in which  $S_{ds,b}(\omega, \theta)$  is the spectrum of bottom shear stress;  $\omega$  is the wave frequency;  $\theta$  is the wave direction;  $g$  is the gravity acceleration ( $9.8 \text{ m s}^{-2}$ );  $k$  is the wave number;  $d$  is the total water

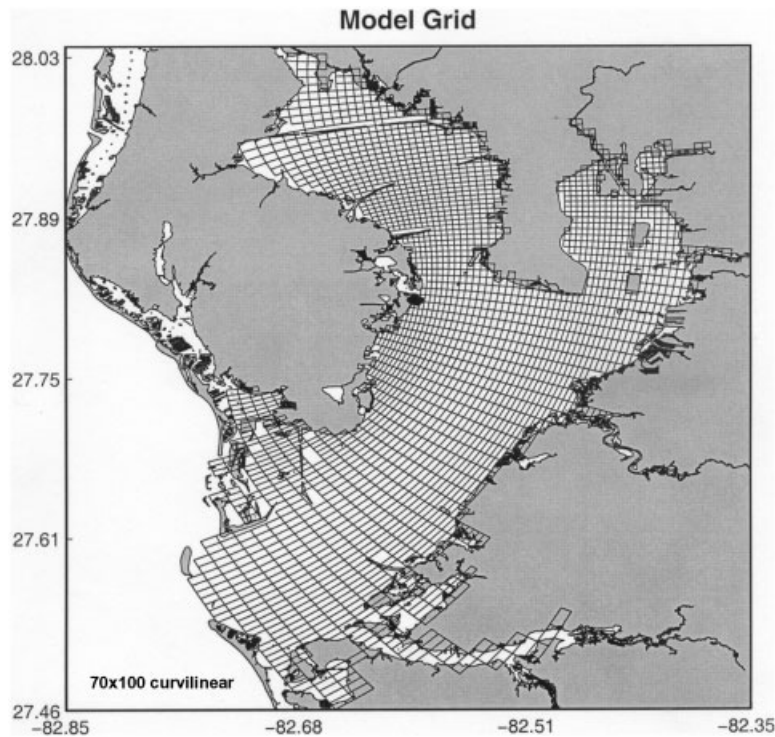


Figure 3. The curvilinear model grid for Tampa Bay contains  $70 \times 100$  cells.

depth;  $E(\omega, \theta)$  is the energy density;  $C_b$  is a bottom friction coefficient that generally depends on the bottom orbital motion represented by  $U_{\text{rms}}$

$$U_{\text{rms}}^2 = \int_0^{2\pi} \int_0^\infty \frac{\omega^2}{\sinh^2(kd)} E(\omega, \theta) d\delta d\theta \quad (2)$$

where  $U_{\text{rms}}$  is the root mean square bottom orbital velocity, which is taken equal to the current at the bed  $U_b$ , will be used for calculating bottom shear stresses and thus total load and bed load of fine sand in Tampa Bay. Hasselmann *et al.* [35] found from the results of the JONSWAP experiment  $C_b = 0.038 \text{ m}^2 \text{ s}^{-3}$  for swell conditions. This value will be cautiously applied to Tampa Bay. There are absolutely no wave measurements available within the Tampa Bay.

The Tampa Bay SWAN uses a high-resolution grid with  $70 \times 100$  cells in a curvilinear domain (Figure 3). A total of 2244 cells are computationally active. The dimensions of active cells range from 2240 to 308 m, with a mean of 668 m. The high-resolution grid will aid in understanding the details of sediment transport. The mean cell area is  $0.425 \text{ km}^2$ , so that the potential or magnitude of fine sand resuspension throughout the Tampa Bay could be better understood. Since the predominant wind direction in Tampa Bay is from the northeast, we simulated the bottom wave-orbital velocity maximum,  $U_b$ , for two idealized winds of 10 and  $20 \text{ m s}^{-1}$  from northeast.

### 3. FINE SAND TRANSPORT MODEL

Two quantities, bed load and total load of fine sand, were modelled because of non-cohesive sediments, mainly fine sands, are present in Tampa Bay. There are several bed load and total load transport formulas available in the literature. The Van Rijn [38] bed load formula and the Engelund–Hansen [39] total load formula were widely used in similar environments in the literature. They were also used for determining the magnitude of fine sand transport in Tampa Bay. The same curvilinear model grid as the SWAN wave model is used for fine sand transport model.

Size classifications of bed sediments are based on Tables 11 (middle Tampa Bay), 12 (Hillsborough Bay) and 13 (Old Tampa Bay) in [9]. Medium particle size  $D_{50} = 130\text{--}150 \mu\text{m}$  for bed sand was used throughout Tampa Bay. The value of the bottom roughness length  $z_0$  for fine sand bed (there were sand ripples present) in Tampa Bay was set to be 0.005 m, because it is not possible to determine the spatial variability in roughness length  $z_0$ . 0.005 m for roughness length  $z_0$  was used throughout Tampa Bay. The model was run with uniform density of sea water ( $1028 \text{ kg m}^{-3}$ ). The Manning's coefficient  $n$  is set equal to 0.025 as used by Goodwin [15].

#### 3.1. Bed load of fine sand

The Van Rijn [38] formula is used for calculating bed load of fine sand in Tampa Bay

$$Q_{\text{bed}} = 0.053 \left[ \left( \frac{\rho_s}{\rho_w} - 1 \right) g \right]^{0.5} D_{50}^{1.5} D_*^{-0.3} T^{2.1} \quad (3)$$

where  $Q_{\text{bed}}$  = the bed load transport rate of fine sand ( $\text{kg m}^{-1} \text{ s}^{-1}$ );  $\rho_s$  = the density of suspended sediment ( $\text{kg m}^{-3}$ );  $\rho_w$  = the density of sea water ( $\text{kg m}^{-3}$ ),  $1028 \text{ kg m}^{-3}$  is used;  $D_*$  is the sand

particle parameter

$$D_* = D_{50} \left[ \left( \frac{\rho_s}{\rho_w} - 1 \right) g / (v^2) \right]^{1/3} \tag{4}$$

where  $v$  is the kinematic viscosity;

In Equation (3),  $T$  is the bed shear stress parameter

$$T = (\tau - \tau_{cr}) / \tau_{cr} \tag{5}$$

$\tau'$  is the effective bed shear stress ( $\text{N m}^{-2}$ )

$$\tau' = \rho g [u / C']^2 \tag{6}$$

where  $\rho = \rho_w$ ;  $u$  is the depth-averaged current velocity ( $\text{m s}^{-1}$ ), which was taken equal to  $U_b$  in Equation (2);  $C'$  is the Chezy's coefficient due to particle friction;  $\tau_{cr}$  is the bed critical shear stress according to Shields [40]

$$\tau_{cr} = (\rho_s - \rho_w) g D_{50} \theta_{cr} \tag{7}$$

where  $\theta_{cr}$  is the Shields parameter determining a value for the critical mobility parameter based on the Shields [40] diagram

$$\begin{aligned} \theta_{cr} &= 0.24(D_*)^{-1}, & D_* < 4.0 \\ \theta_{cr} &= 0.14(D_*)^{-0.64}, & 4.0 < D_* < 10.0 \\ \theta_{cr} &= 0.04(D_*)^{-0.10}, & 10.0 < D_* < 20.0 \\ \theta_{cr} &= 0.013(D_*)^{0.29}, & 20.0 < D_* < 150.0 \\ \theta_{cr} &= 0.055, & D_* > 150.0 \end{aligned}$$

### 3.2. Total load of fine sand

Due to the hydrodynamic complexity, no unique sediment transport formula has a wide range of application in the marine environment. For the suspended load on the sandy beach, use is frequently made of the energetics approach of Bailard [41], which relates sediment flux to near-bed fluid velocity, assuming an equilibrium vertical distribution of sediment concentration. Bailard [41] is also for bed and suspended load and can include the effects of waves and bed slopes. Bailard [41] has the advantage of simplicity in the marine environment, but it has two disadvantages: (1) of not being able to model the net sediment transport rate which results from certain types of wave asymmetry [42]; (2) only for coastal environments which may have strong external currents. Applying the Bailard [41] model however, to Tampa Bay with complex sea beds can possibly result in unrealistic sediment transport predictions with the model also only being applicable when no currents exist during the slack water periods. Therefore, an alternative formula for total load of fine sand, i.e. Engelund–Hansen [39], is used for Tampa Bay.

Although the Engelund and Hansen [39] equation is designed for a river environment [43]. In our present Tampa Bay study, it is assumed that the wind wave-induced current is approximately steady. The Engelund and Hansen [39] formula has been used very cautiously in the Tampa Bay. Local equilibrium of fine sand transport rate is assumed for Tampa Bay. The Engelund–Hansen

Table I. Summary of parameters used in the models.

The kinematic viscosity $\nu$	$1.47 \times 10^{-6} \text{ m}^2 \text{ s}^{-1}$
Roughness length $z_0$	0.005 m
The Chezy value $Ch$	0.025
The Manning's coefficient $n$	0.025
Density of suspended sediment $\rho_s$	$2650 \text{ kg m}^{-3}$
Density of seawater $\rho_w$	$1028 \text{ kg m}^{-3}$
Medium particle size $D_{50}$	150 $\mu\text{m}$
$D_{90}$	130 $\mu\text{m}$

[39] formula is employed in estimating the total load (bed load and suspended load) of fine sand in Tampa Bay.

$$Q_{\text{total}} = 5.0 \times \left\{ 0.05 \left/ \left[ g^3 \left( \frac{\rho_s}{\rho_w} - 1 \right)^2 D_{50} \right] \right. \right\} \times (\sqrt{g} \times U/Ch)^5 \times C'^2 \quad (8)$$

where  $Q_{\text{total}}$  is the total load of fine sand ( $\text{kg m}^{-1} \text{ s}^{-1}$ );  $D_{50}$  = the medium diameter of bed sediments (m);  $U$  is the current velocity ( $\text{m s}^{-1}$ ) in calculation, it was set equal to the rms bottom orbital current speed, i.e.  $U \approx U_b$ ;  $Ch$  is the Chezy value, in reality it depends on the water depth  $h$ , the bottom roughness and flood/ebb differences and lag effects in turbulent intensity; for the sake of simplicity, however, the Chezy value will be assumed constant, 0.025 is used throughout Tampa Bay (Table I);  $C'$  is the Chezy's coefficient due to particle friction ( $\text{m}^{0.5} \text{ s}^{-1}$ ):

$$C' = 18.0 \ln(12.0h/3D_{90}) \quad (9)$$

where  $h$  is the water depth (m), high-resolution bathymetry is used throughout Tampa Bay;  $D_{90}$  is the sediment diameter with 90% finer (m), 130  $\mu\text{m}$  is used throughout Tampa Bay.

For a constant Chezy value, the bottom friction is generally constant with water depth. A 'simple' Chezy model would represent the situation often found where shallow coastal waters are relatively smooth and channels and deeper areas exhibit wave ripples like Tampa Bay. Similarly, Lin and Chandler-Wilde [44] assumed a constant Chezy value throughout the whole estuary. In the present study, a constant Chezy value can be used for Tampa Bay during the slack water period. In the future studies, several constant Chezy values should be used to calibrate the model. However, it is currently beyond the scope of this paper.

The limitations and results of our model due to the approximations are mainly two fold: (1) either over-estimations or under-estimations of bottom shear stresses; (2) either over-estimations or under-estimations of bed load and total load of fine sand in the different part of the Tampa Bay.

## 4. RESULTS AND DISCUSSIONS

### 4.1. Wind wave-induced bottom orbital currents

Tampa Bay is very near the shoreface, where wave-driven transport is more common. Our discussions have been made within the context of the shoreline rather than within the open bay. Wind wave-induced bottom orbital currents can be significant mechanism for bottom fine sand transport in Tampa Bay. Several frontal systems pass through Tampa Bay and generate strong



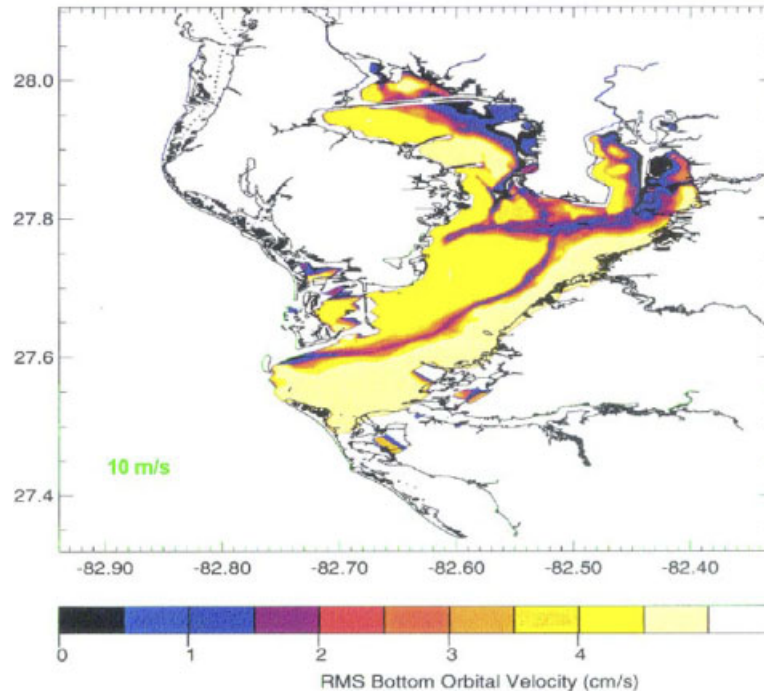


Figure 4. Modelled wind wave-induced bottom orbital speed for steady northeasterly winds of  $10 \text{ m s}^{-1}$ .

winds that increase wave action and can resuspend fine sands. As shown in Figures 4 and 6, wind wave-induced bottom orbital velocities for northeasterly winds of  $10$  and  $20 \text{ m s}^{-1}$  have similar patterns with large differences in magnitude. Low bottom orbital velocities for winds of  $10$  and  $20 \text{ m s}^{-1}$  are present in the most part of Hillsborough Bay and the northeastern Old Tampa Bay (Figure 4). These low bottom orbital velocities might have resulted in fine cohesive sediment deposition in the Hillsborough Bay and Old Tampa Bay, as observed by Sheng *et al.* [17] and Schoellhamer [16].

The significant wave heights ranged from  $0.20$  to  $0.65 \text{ m}$ , with typical periods of  $2 \text{ s}$  for steady northeasterly winds of  $10 \text{ m s}^{-1}$ . The significant wave heights ranged from  $0.40$  to  $1.50 \text{ m}$ , with typical periods of  $3 \text{ s}$  for northeasterly winds of  $20 \text{ m s}^{-1}$ . Schoellhamer [16] observed the waves periods of about  $2.6\text{--}2.8 \text{ s}$  during the storm (winds) on 8–9 March 1990. The bottom orbital current speeds range from  $0.05 \text{ m s}^{-1}$  in the channel (deep regions) to more than  $0.27 \text{ m s}^{-1}$  across the intertidal zone (shallow region), for northeasterly winds of  $10 \text{ m s}^{-1}$  (Figure 4). The bottom velocities ranged from less than  $0.14 \text{ m s}^{-1}$  in the channel (deep regions) to more than  $0.24 \text{ m s}^{-1}$  in the intertidal (shallow regions) zone (Figure 5), for northeasterly winds of  $20 \text{ m s}^{-1}$ . As shown in Figure 5, modelled bottom orbital velocities were generally larger than  $18 \text{ cm s}^{-1}$  in the shallow waters (i.e. intertidal zone). Within the deeper channels, however, modelled bottom orbital currents ranged from  $8$  to  $12 \text{ cm s}^{-1}$ . Modelled bottom orbital velocities apparently increase from the lower Tampa Bay to the middle Tampa Bay to the old Tampa Bay and Hills. This may suggest that the lower Tampa Bay is subject to the stronger incoming wind waves than the other parts of Tampa

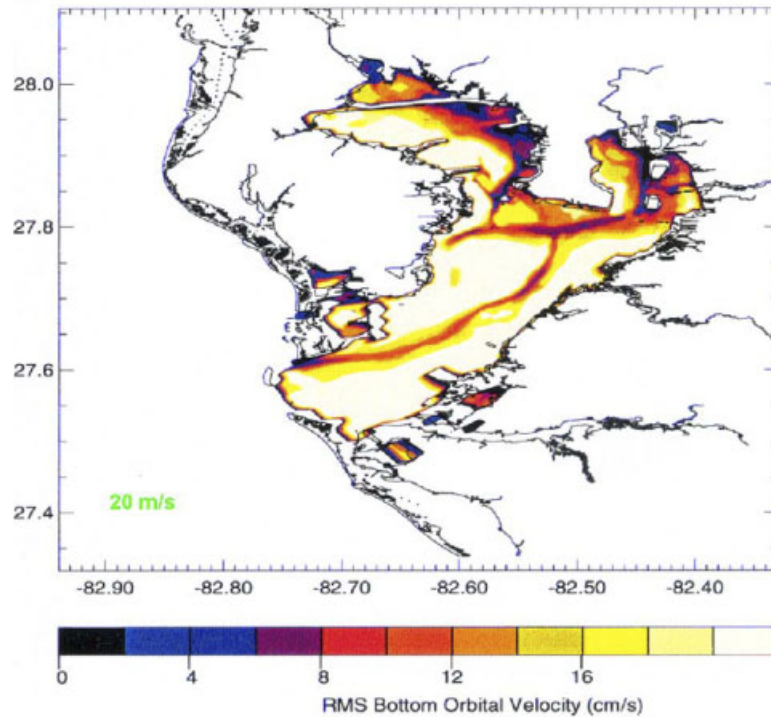


Figure 5. Modelled wind wave-induced bottom orbital speed for steady northeasterly winds of  $20 \text{ m s}^{-1}$ .

Bay. When wind speed increases from  $10 \text{ m s}^{-1}$  (Figure 4) to  $20 \text{ m s}^{-1}$  (Figure 5), as a result, modelled bottom orbital velocities increase 2–3 orders of magnitude (Figure 5). During episodic events, wind wave-induced bottom shear stresses are very effective in causing significant resuspension of non-cohesive sediments in Tampa Bay [16, 17].

#### 4.2. Bed load of fine sand

Modelled results reveal that bed load values were absent for winds of  $10 \text{ m s}^{-1}$  from the northeast. It is suggested that wind wave-induced bottom currents driven by winds of  $10 \text{ m s}^{-1}$  were insufficient to mobilize fine sand beds in Tampa Bay. The calculated sand particle parameter  $D_*$  and Shields parameter  $\theta_{cr}$  are 3.74 and  $6.42 \times 10^{-2}$ , respectively, regardless of wind speeds. However, they may be sufficient to resuspend cohesive sediments in the Hillsborough Bay. Bed load of fine sand driven by northeasterly winds of  $20 \text{ m s}^{-1}$  was present in the southern Middle Tampa Bay and the northwestern Lower Tampa Bay (Figure 6). A real per cent of bottom sands for bed load is 0.57%. In other words, winds of  $20 \text{ m s}^{-1}$  could cause approximately 0.57% of bed load of fine sand. Bed load of fine sand ranged from  $2.48 \times 10^{-8}$  to  $4.67 \times 10^{-5} \text{ kg m}^{-1} \text{ s}^{-1}$  (Figure 6). Bed load of fine sand might be underestimated or overestimated by using the Van Rijn [38] formula. It is not clear how accurate this calculation is. Since there is no fine sand transport measurement data available in Tampa Bay or even similar estuarine and coastal environments, it is not possible

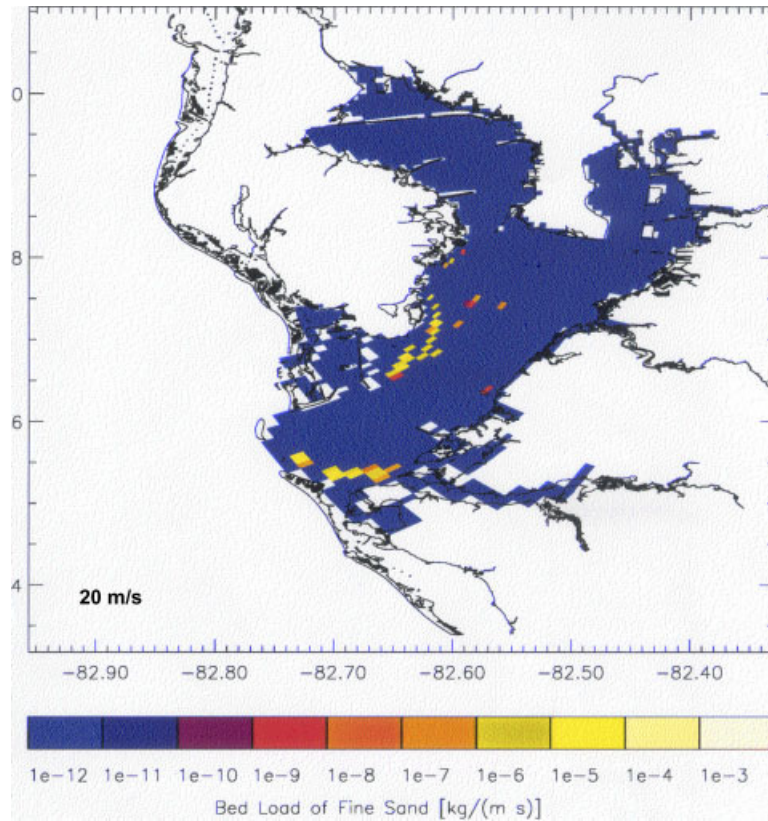


Figure 6. Modelled bed load transport driven by wind wave-induced bottom orbital currents (northeasterly winds of  $20 \text{ m s}^{-1}$ ).

to estimate an approximate error for our calculation based on the Van Rijn [38] formula. However, an approximate error for our calculation using the Van Rijn formula should be expected to roughly range from 15 to 25%, which are within the ranges for alluvial rivers using the Van Rijn formula [45].

However, wind wave-induced bottom orbital velocity superposed on those computed by the tidal hydrodynamic model [27, 28], the combined currents might be sufficient to mobilize more fine sand bed in Tampa Bay. In the future, the combined wave and current shear stresses must be calculated. Non-linear interaction of waves and currents during winter storms could enhance the bottom shear stresses and resuspend fine sand in Tampa Bay.

Many numerical models of estuarine tidal circulation and wind-wave have traditionally been run separately, while estuarine sediment transport models have typically only considered tidal current-induced transport, neglecting wave-induced transport. Physics of estuarine coupled waves, currents and sediments are not fully understood, and especially wave-current coupling in the bottom boundary layer is still a challenge. Coupled numerical modelling has been limited to simplified models or idealized wave and current fields, due to the performance limitations of sequential

computer systems. Thus, we argue that it would be very difficult to couple our SWAN model and suspended load model with an ECOM model of Tampa Bay [27, 28].

#### 4.3. Total load of fine sand

The magnitude of fine sand transport driven by wind wave-induced bottom currents (Figures 4 and 5) in Tampa Bay is shown in Figures 7 and 8. Spatial gradients in total load of fine sand would cause erosion and accretion of the sand bed in Tampa Bay. High total loads of fine sand are present in the southwestern Old Tampa Bay, the northwestern Middle Tampa Bay and the southeastern Lower Tampa Bay (Figures 7 and 8). As expected, total loads of fine sand are very low along the channel (deep region) in Tampa Bay and north of Bay (Figures 7 and 8). Very low total loads of fine sand are also present in Hillsborough Bay (Figure 7). Calculated total loads of fine sand are shown in Figures 7 and 8. Total loads of fine sand ranged from  $2.26 \times 10^{-10}$  to  $1.05 \times 10^{-5} \text{ kg m}^{-1} \text{ s}^{-1}$  for northeasterly winds of  $10 \text{ m s}^{-1}$  (Figure 7) and from  $2.46 \times 10^{-5}$  to  $3.21 \times 10^{-5} \text{ kg m}^{-1} \text{ s}^{-1}$  for northeasterly winds of  $20 \text{ m s}^{-1}$  (Figure 8). There is a strong correlation between the patterns of modelled wind wave-induced bottom orbital currents and total loads of fine sand.

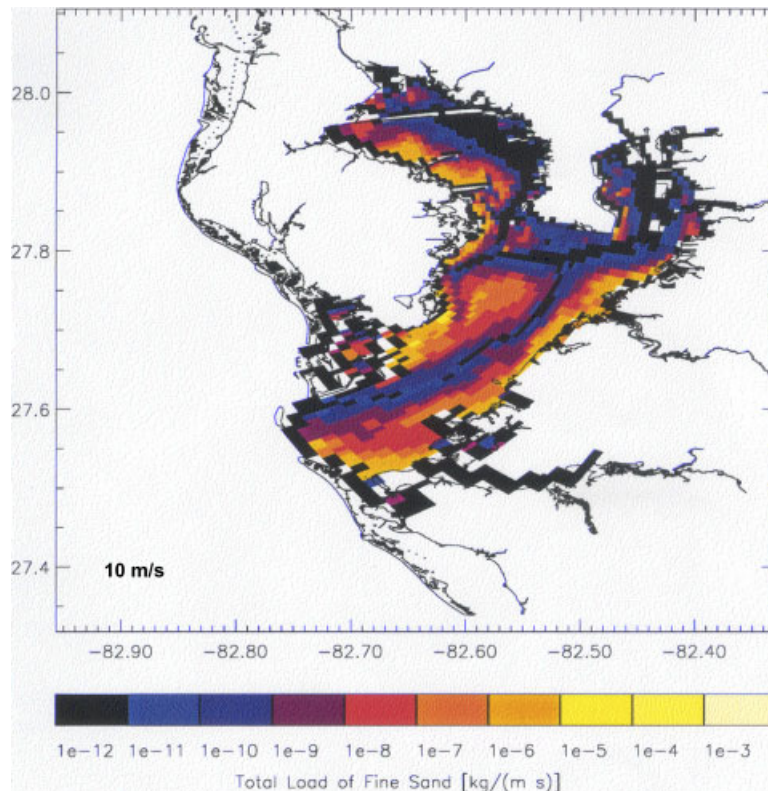


Figure 7. Modelled total load of fine sand driven by wind wave-induced bottom orbital currents (northeasterly winds of  $10 \text{ m s}^{-1}$ ).



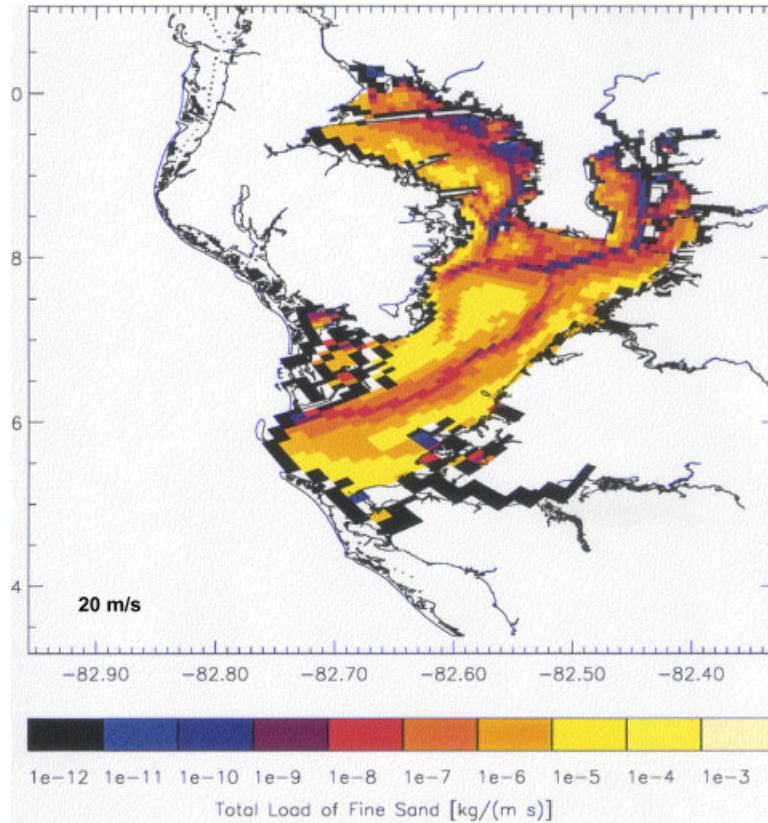


Figure 8. Modelled total load of fine sand driven by wind wave-induced bottom orbital currents (northeasterly winds of  $20 \text{ m s}^{-1}$ ).

It is noted that bed load and total load of fine sands might be underestimated or overestimated because of several assumptions. For example, these simulations assume a uniform particle size of bed sediments. However, it is difficult to know how much loads would have been underestimated or overestimated owing to a lack of observational data. It is clear that the wind wave-induced bottom current is one transport mechanism for fine sand in Tampa Bay. Maximum suspended-solids concentration could be up to  $40 \text{ mg l}^{-1}$  in winter in Old Tampa Bay [16]. It should be emphasized that the wave, bed load, and total load values presented throughout the paper are modelled. There is especially a tendency to present sediment transport as a fact, rather than an estimate.

## 5. CONCLUSIONS

Although this modelling study is based upon several assumptions, several preliminary conclusions can be drawn from this study. Magnitude of potential fine sand transport is determined by modelling

bed load and total load of fine sand in Tampa Bay. The bottom orbital current speeds range from  $0.05 \text{ m s}^{-1}$  in the deep channel to more than  $0.27 \text{ m s}^{-1}$  across the intertidal zone for northeasterly winds of  $10 \text{ m s}^{-1}$ . Wind wave-induced bottom orbital speeds range from less than  $0.14 \text{ m s}^{-1}$  in the deep channel to more than  $0.39 \text{ m s}^{-1}$  in the shallow regions for northeasterly winds of  $20 \text{ m s}^{-1}$ . Total loads of fine sand range from  $2.26 \times 10^{-10}$  to  $1.05 \times 10^{-5} \text{ kg m}^{-1} \text{ s}^{-1}$  and from  $2.46 \times 10^{-5}$  to  $3.21 \times 10^{-5} \text{ kg m}^{-1} \text{ s}^{-1}$  for northeasterly winds of 10 and  $20 \text{ m s}^{-1}$ , respectively.

#### ACKNOWLEDGEMENTS

This manuscript was prepared during Z. Shi's stay (November 2001 to February 2002) as a visiting scientist at the Laboratory of Ocean Modelling, College of Marine Science, University of South Florida, St. Petersburg, U.S.A. Z. Shi acknowledges financial support from the Ministry of Education of People's Republic of China (the PhD Supervisor Program 2001-393, Division of International Collaboration and Exchange). Special thanks to Amanda Frick (GIS Coordinator, USGS, St. Petersburg) for assistance in obtaining sediment data. This work was supported in part by the USGS Center for Coastal Geology and Regional Marine Studies, the Shanghai Rising-Star Program (03QMH1408) and the National Science Fund for Distinguished Young Scholars of China (Estuarine and Coastal Sciences 40225014). Reviewers are thanked for their constructive comments.

#### REFERENCES

1. Myrhaug D, Slaattelid OH, Lambrakos KF. Seabed shear stresses under random waves: predictions vs estimates from field measurements. *Ocean Engineering* 1998; **25**(10):907–916.
2. Sanford LP, Panageotou W, Halka JP. Tidal resuspension of sediments in northern Chesapeake Bay. *Marine Geology* 1991; **97**:87–103.
3. Shi Z, Ren LF, Hamilton LJ. Acoustic profiling of fine suspension concentration in the Changjiang Estuary. *Estuaries* 1999; **22**(3A):648–656.
4. Lavalle JW, Young RA, Swift DJP, Clarke TL. Near-bottom sediment concentration and fluid velocity measurements on the inner continental shelf, New York. *Journal of Geophysical Research* 1978; **83**:6052–6062.
5. Ward LG, Kemp WM, Boynton WR. Influence of waves and seagrass communities on suspended particulates in an estuarine embayment. *Marine Geology* 1984; **59**:85–103.
6. Sanford LP. Wave-forced resuspension of upper Chesapeake Bay muds. *Estuaries* 1994; **17**(1B):148–165.
7. Lou J, Ridd PV. Wave-current bottom shear stresses and sediment resuspension in Cleveland Bay, Australia. *Coastal Engineering* 1996; **29**:169–186.
8. Mei CC, Chain CM. Dispersion of suspended particles in wave boundary layers. *Journal of Physical Oceanography* 1994; **24**(12):2479–2495.
9. Mei CC, Fan SJ, Jin KR. Resuspension and transport of fine sediments by waves. *Journal of Geophysical Research (Oceans)* 1997; **102**(C):15807–15821.
10. Lin BL, Falconer RA. Numerical modeling of three-dimensional suspended sediment for estuarine and coastal waters. *Journal of Hydraulic Research* 1996; **34**(4):435–455.
11. Booth JG, Miller RL, McKee BA, Leathers RA. Wind-induced bottom sediment resuspension in a microtidal coastal environment. *Continental Shelf Research* 2000; **20**:785–806.
12. Signell DM, List JH, Farris A. Bottom currents and sediment transport in Long Island Sound: a modeling study. *Journal of Coastal Research* 2000; **16**(3):551–566.
13. Brooks GR, Doyle LJ. Recent sedimentary development of Tampa Bay, Florida: a microtidal estuary incised into Tertiary platform carbonates. *Estuaries* 1998; **21**(3):391–406.
14. Wang PF, Martin J, Morrison G. Water quality and eutrophication in Tampa Bay, Florida. *Estuarine, Coastal and Shelf Science* 1999; **49**(1):1–20.
15. Goodwin CR. Tidal-flow, circulation, and flushing changes caused by dredge and fill in Tampa Bay, Florida. *U.S. Geological Survey Water-Supply Paper* 1987; **2282**:1–88.
16. Schoellhamer DH. Sediment resuspension mechanisms in Old Tampa Bay, Florida. *Estuarine, Coastal and Shelf Science* 1995; **40**(6):603–620.

17. Sheng YP, Chen XJ, Yassuda A. Wave-induced sediment resuspension and mixing in shallow waters. In *Proceedings of the 24th International Conference on Coastal Engineering*, Edge BL (ed.). ASCE: New York, 1995; 3281–3294.
18. Weisberg RH, Williams RG. Initial findings on the circulation of Tampa Bay. In *Proceedings of the Tampa Bay Area Scientific Information Symposium*, Treat S, Clark P (eds), vol. 2. Tampa, FL, 27 February–1 March, 1991; 49–66.
19. Sheng YP, Yassuda E, Chen XJ. On hydrodynamics and water quality dynamics in Tampa Bay. In *Proceedings of Tampa Bay Area Scientific Information Symposium—Applying Our Knowledge*, Treat SF (ed.), vol. 3. Tampa Bay Regional Planning Council, FL, U.S.A., 1997; 295–314.
20. Lewis RR, Durako MJ, Moffler MD, Phillips RC. Seagrass meadows of Tampa Bay—a review. In *Proceedings of the Tampa Bay Area Scientific Information Systems*, Treat SF, Simon JL, Lewis III RR, Whitman Jr RL (eds). Tampa, FL, Bellwether Press: Minneapolis, 1985; 210–216.
21. Fonseca MS, Kenworthy WJ, Courtney FX. Developments of planted seagrass beds in Tampa Bay, Florida, U.S.A., 1. Plant components. *Marine Ecology Progress Series* 1996; **132**(1–3):127–139.
22. Schoellhamer DH. Observations of sediment resuspension in Old Tampa Bay, Florida. *Proceedings of the 1990 National Conference on Hydraulic Engineering*, San Diego, California, ASCE, New York, 1990; 51–56.
23. Levesque VA, Schoellhamer DH. Summary of sediment resuspension monitoring activities, Old Tampa Bay and Hillsborough Bay, Florida, 1988–1991. *U.S. Geological Survey Water-Resources Investigations Report 94-4081*, 1995.
24. Galperin B, Blumberg AF, Weisberg RH. A time-dependent three-dimensional model of circulation in Tampa Bay. In *Proceedings of the Tampa Bay Area Scientific Information Symposium*, Treat S, Clark P (eds), vol. 2. Tampa, FL, 27 February–1 March, 1991, 1992; 77–98.
25. Hess K, Bosley K. Techniques for validation of a model for Tampa Bay. *Proceedings of the 2nd International Conference on Estuarine and Coastal Modeling*, ASCE, Tampa, FL, 13–15 November 1991, 1992; 83–94.
26. Hess KW. *Modeled Hydrodynamics. Tampa Bay Oceanography Project. Physical Oceanographic Synthesis, NOS OES002*, NOAA, Silver Spring, MD, 1993; 143–162.
27. Vincent M, Burwell D, Luther M, Galperin B. Real-time data acquisition and modeling in Tampa Bay. In *Proceedings of the 5th International Conference on Estuarine and Coastal Modeling*, Spaulding M, Blumberg A (eds). ASCE: Alexandria, VA, U.S.A., 22–24 October 1997, 1998; 427–440.
28. Vincent M, Burwell D, Luther ME. Tampa Bay nowcast-forecast system. In *Proceedings of the 6th International Conference on Estuarine and Coastal Modeling*, Spaulding M, Butler H (eds). ASCE: New Orleans, LA, U.S.A., 3–5 November 1999, 2000; 765–780.
29. Galperin B, Blumberg AF, Weisberg RH. The importance of density driven circulation in well mixed estuaries: the Tampa experience. *Proceedings of the 2nd International Conference on Estuarine and Coastal Modeling*, Tampa, FL, 13–15 November 1991, 1992; 332–343.
30. Shi Z, Meyers S, Luther ME. Modeling of wind wave-induced bottom currents and fine sand transport in Tampa Bay, Florida. *Proceedings of the International Conference on Estuaries and Coasts*. Hangzhou, Zhejiang University Press: China, 9–11 November 2003; 865–871.
31. Booij N, Ris RC, Holthuijsen LH. A third-generation wave model for coastal regions. Part I. Model descriptions and validation. *Journal of Geophysical Research* 1999; **104**(C4):7649–7666.
32. Ris RC, Holthuijsen LH, Booij N. A third-generation wave model for coastal regions 2 verification. *Journal of Geophysical Research* 1999; **104**:7667–7681.
33. Holthuijsen LH, Booij N, Herbers THC. A prediction model for stationary, short-crested waves in shallow water with ambient currents. *Coastal Engineering* 1989; **13**:23–54.
34. Gorman RM, Laing AK. Wave hindcast for the New Zealand region: nearshore validation and coastal wave climate. *New Zealand Journal of Marine and Freshwater Research* 2003; **37**:567–588.
35. Hasselmann K, Bennett TP, Bocaws E, Carlson H, Cartwright DE, Enke K, Ewing JA, Gienapp H, Hasselmann DE, Kruseman P, Meerburg A, Muller P, Olbers DJ, Richter K, Sell W, Walden H. Measurement of wind-wave growth and swell decay during the Joint North Sea Wave Project (JONSWAP). *Dtsch. Hydrograph. Z.* 1973; **A8**(Suppl. 12).
36. Collins JJ. Prediction of shallow water spectra. *Journal of Geophysical Research* 1972; **77**(15):2693–2707.
37. Madsen OS, Poon YK, Graber HC. Spectra wave attenuation by bottom friction: theory. *Proceedings of the 21st International Conference on Coastal Engineering*, ASCE, New York, 1988; 492–504.
38. Van Rijn LC. Sediment transport. Part I: bed load transport. *Journal of Hydraulic Engineering* 1984; **110**: 1431–1456.

39. Engelund F, Hansen E. *A Monograph on Sediment Transport in Alluvial Streams*. Copenhagen Technical Press: 1972.
40. Shields A. Anwendung der Aechlichkeitsmechanik und der Turbulenz Forschung auf die Geschiebebewegung. *Mitteilungen der Pruessischen Versuchsanstalt fuer Wasserbau and Schiffbau*, Berlin, 1936.
41. Bailard JA. An energetics total load sediment transport model for a plane sloping beach. *Journal of Geophysical Research* 1981; **86**:10938–10954.
42. Nielsen P. *Coastal Bottom Boundary Layers and Sediment Transport*. World Scientific: Singapore, 1992; 122.
43. Li MZ, Amos CL. SEDTRANS96: the upgraded and better calibrated sediment-transport model for continental shelves. *Computers and Geosciences* 2001; **27**:619–645.
44. Lin BL, Chandler-Wilde SN. A depth-integrated 2D coastal and estuarine model with conformal boundary-fitted mesh generation. *International Journal for Numerical Methods in Fluids* 1996; **23**:819–846.
45. Wu W, Wang SSY, Jia Y. Nonuniform sediment transport in alluvial rivers. *Journal of Hydraulic Research* 2000; **38**(6):427–434.